

Supporting information for

**Supramolecular organization of a H-bonded perylene
bisimide organogelator determined by transmission electron
microscopy, grazing incidence X-ray diffraction and polarized
infra-red spectroscopy.**

Alexandru Sarbu¹, Patrick Hermet⁴, David Maurin³, David Djurado², Laure
Biniek¹, Morgane Diebold¹, Jean-Louis Bantignies³, Philippe Mésini¹ and
Martin Brinkmann¹

(1) Université de Strasbourg, CNRS, ICS UPR22, F67000 Strasbourg, France

(2) UMR SPrAM 5819 (CEA-CNRS-UJF) and SP2M, CEA Grenoble/INAC, 38054,
Grenoble Cedex, France

(3) Laboratoire Charles Coulomb, Université de Montpellier, 4, place E. Bataillon,
34095 Montpellier, France

(4) Institut Charles Gerhardt Montpellier, UMR 5253 CNRS-UM-ENSCM, Place E.
Bataillon, 34095 Montpellier, France, Institut Laue Langevin, 6 Rue Jules
Horowitz, B.P. 156, 38042 Grenoble

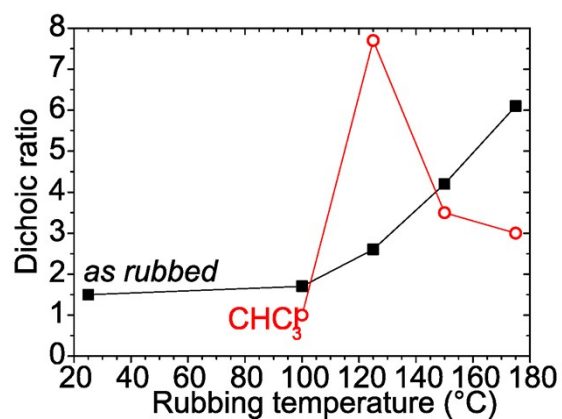


Figure S1. Evolution of the dichroic ratio of rubbed PBI-C10 films as a function of rubbing temperature (full squares). The evolution of the dichroic ratio is also shown for the films rubbed at various temperatures and subsequently exposed (30 min) to a saturated atmosphere of CHCl_3 (red open circles). The line in the plots are guide to the eye.

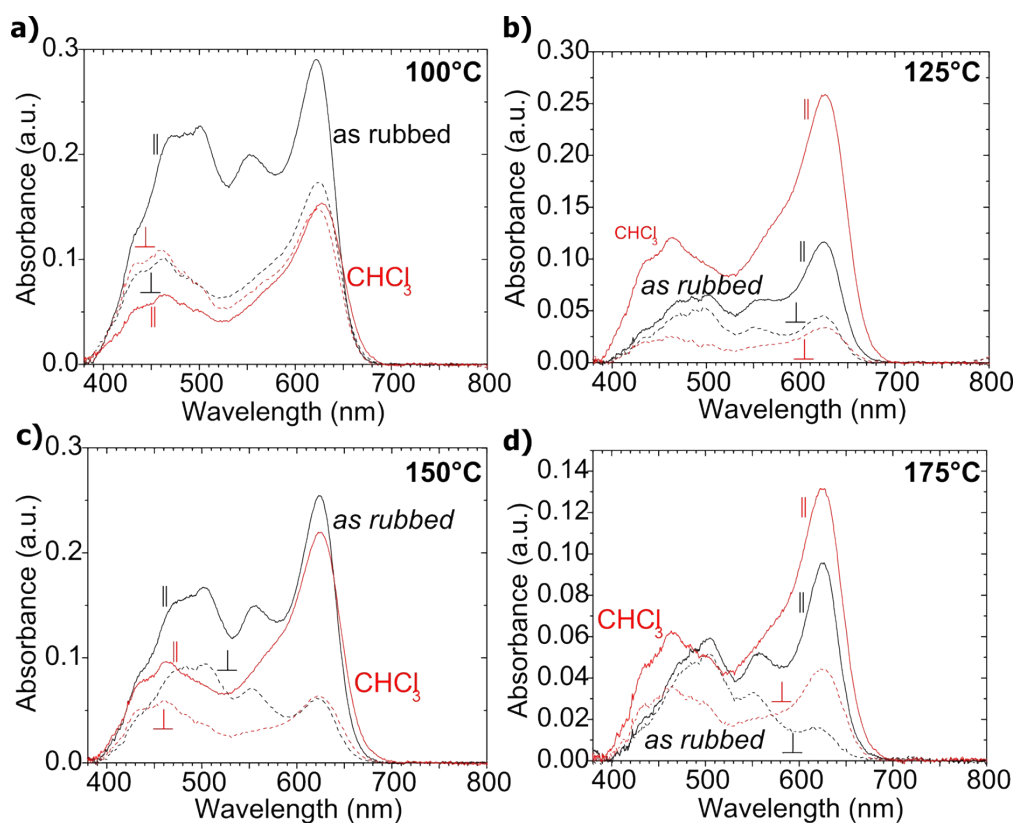


Figure S2. Evolution of the polarized UV-vis absorption spectrum of thin films of PBI-C10 oriented by mechanical rubbing at different temperatures for parallel (full lines) and perpendicular (dotted lines) orientation of the incident light with respect to the rubbing direction. The spectra of the films after solvent vapor annealing in CHCl_3 (30min) are also shown in red for both orientations.

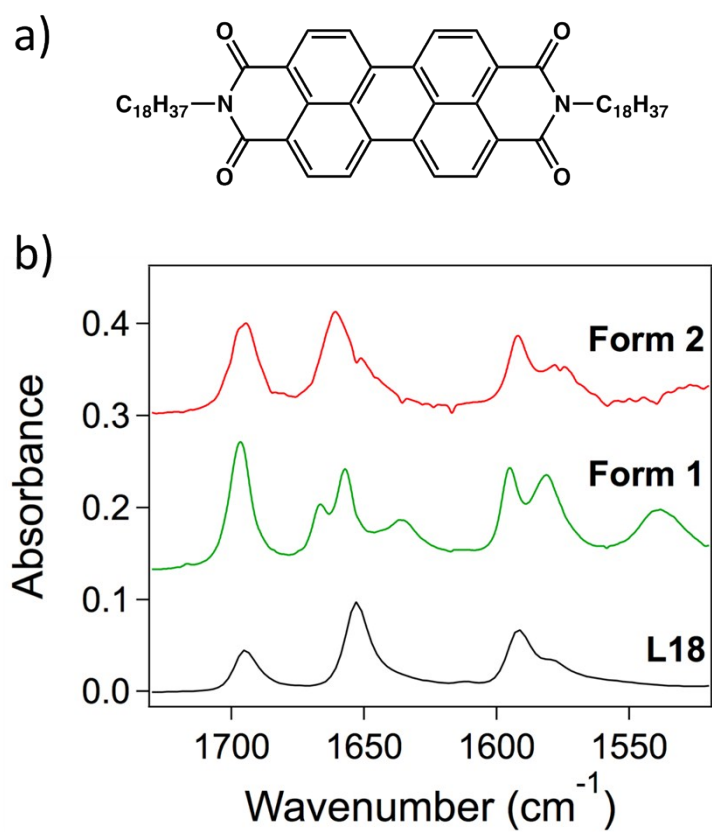


Figure S3. Molecular structure of the L18 PBI analogue (a) with linear solubilizing alkyl chains and (b) comparison of the FTIR spectra of form I, form II and L18 for the assignment of imide and amide bands. L18 has no amide groups.

Table S1. Calculated and experimental mid-IR band positions of PBI-C10 form I with their proposed assignment. The middle infrared bands (3600 – 1550 cm^{-1}) show a significant experimental dichroism. The polarization of the calculated bands is given in the frame of the PBI core (x axis: short axis of the PBI core, y axis: long axis of the PBI, z axis: normal to the PBI core). No orientation for the vibrational modes of the amide groups in the molecular frame are given because the model cannot predict the exact molecular conformation of the PBI-C10 molecules in form I, hence the relative orientation of the amide groups to the PBI core. The lack of interactions induces that the IR active amide A modes are well resolved compared to the experimental ones engaged in H-bonding along the rubbing direction.

$\bar{\nu}$ (cm^{-1}) Exp.	$\bar{\nu}$ (cm^{-1}) calc.	Assignment	Orientation of transition dipole in the molecular frame ^a	Maximum of mode intensity with respect to the rubbing direction
3317	3502	Amide A	-	//
	3445			
	3430			
3250	3322	Amide A	-	//
1697(a)	1689	Imide ($\nu_s \text{CO}$)	// y	//
1668(b)	1675	Amide I (WA1)	-	\perp
	1668			
1660(c)	1659	Imide $\nu_{as} \text{CO}$	(x, z)	\perp
1635(d)	1647	Amide I (SA1)	-	//
1595(e)	1621	Perylene ν_{cc}	// y	//
1581(f)	1597	Perylene ν_{cc} Benz. ν_{cc}	(x,y)	//
	1592			
	1586			
	1580			

Table S2 : Dipole moment coordinates (P_x , P_y , P_z) for IR active vibrations. x : short axis of the perylene, y : long axis of the peryle and z : perpendicular to the aromatic core). The angles q_{yP} , q_{zP} , q_{xP} are between the molecular axes and the dipole moment for a given IR active vibration.

ν (cm ⁻¹)	P_x	P_y	P_z	q_{yP} (°)	q_{xP} (°)	q_{zP} (°)	Assign.
1689	-0.30	0.76	-0.17	24	111	102	ν_s CO imide
1675	0.25	-0.71	-0.11	159	71	98	Amide 1
1668	-0.04	-0.49	-0.20	158	94	112	Amide 1
1659	-0.84	-0.2	-0.42	102	151	116	ν_{as} (CO)imide
1647	-0.15	-0.40	-0.15	152	109	109	Amide 1
1621	-0.03	0.84	-0.09	6	92	96	Aro. core. $\nu_{C=C}$
1597	0.13	0.30	-0.22	40	71	124	Aro core. $\nu_{C=C}$ + benz $\nu_{ip}C=C$
1592	0.08	-0.31	0.06	162	76	79	$\nu_{C=C}$
1586	-0.07	-0.17	0.01	157	112	87	benz $\nu_{ip}C=C$

Table S3. Main reflections of form II of PBI-C10 observed in the ED pattern of Figure 6 and corresponding indexation using the determined trigonal unit cell (see text).

Indexation of reflection	d_{hkl} (Å)
1 0 0	53.6±1.2
2 0 0	26.8±0.8
3 0 0	17.7±0.6
4 0 0	13.2±0.4
6 0 0	8.8±0.2
1 0 1	47.0±1.0
2 0 1	25.4±0.8
3 0 1	17.4±0.6
7 0 1	7.5±0.2
3 0 2	16.6±0.5
4 0 2	12.6±0.3
4 0 19	4.7±0.1
5 0 20	4.7±0.1
0 0 21	4.6±0.1
2 0 21	4.6±0.1
5 0 21	4.3±0.1
0 0 22	4.4±0.1
10 0 19	3.6±0.1

Figure S4 shows some characteristic ED patterns for the films rubbed at 125°C and annealed at 190°C for 5 hrs. They correspond to different areas on the films and show some differences, especially in the low angle region (see enlarged part of Figure S4.b). The ED patterns display a large number of very sharp low-angle reflections indicative of long-range supramolecular order and some broader high angle reflections characteristic of molecular stacking order. As shown hereafter, all observed patterns correspond to the same structure but with different contact planes on the substrate. Table S2 lists the most characteristic reflections of this polymorph.

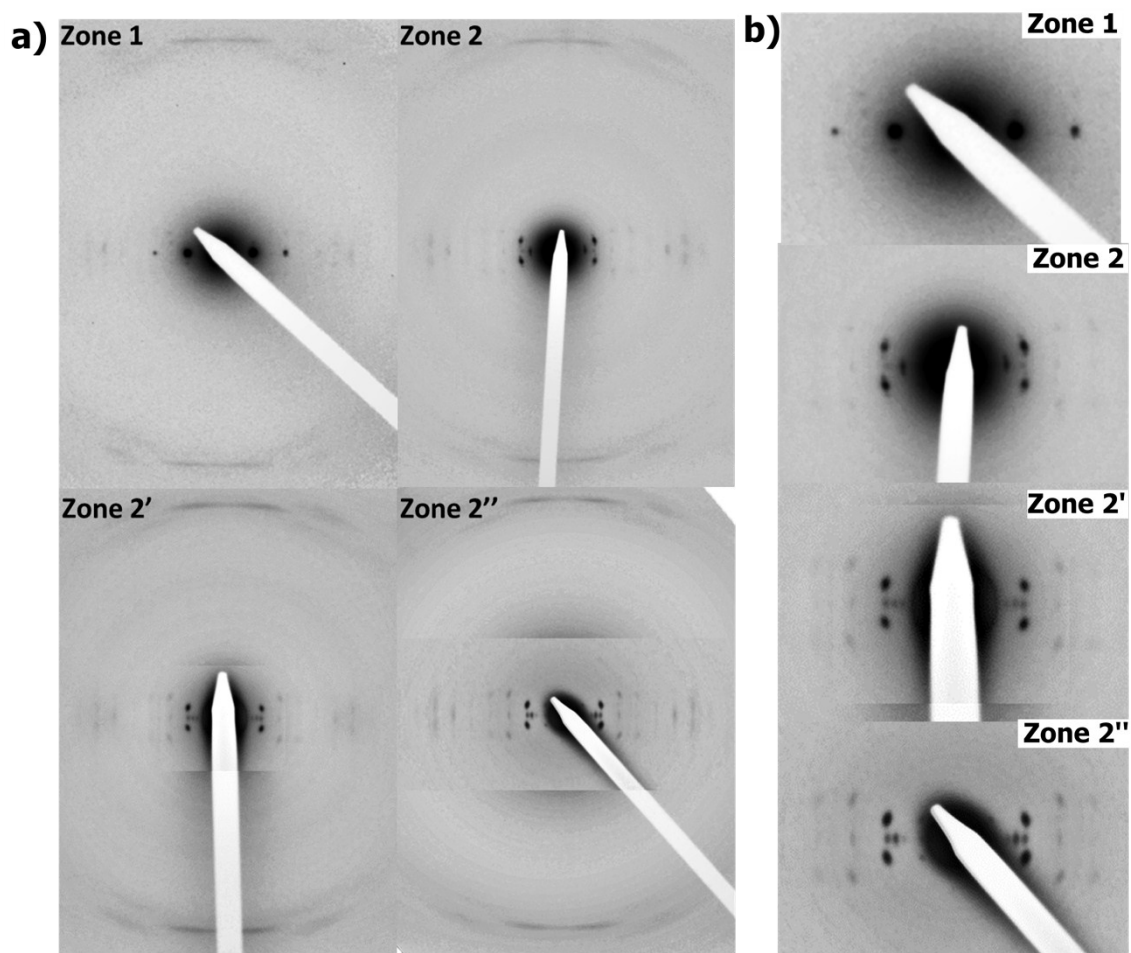


Figure S4. a) Various ED patterns observed for a PBI-C10 form II oriented thin film and corresponding to different areas on the sample. The low angle part of the patterns is

represented with a different intensity scale to highlight some of the low angle reflections. Zone 1 is significantly different from the 2, 2' and 2'' areas. The rubbing axis is vertical for all the images. b) Enlarged view of the low angle part of the ED patterns.

Structural modeling of the trigonal structure of form II of PBIC10.

Several characteristics of the ED pattern in Figure 6 help orient the modeling of the molecular packing in form II:

- i) the intensity of the main reflection in the 21st layer is off-meridional,
- ii) the most intense reflections in the layer lines close to the 21st layer line are located on a line that makes an angle of 63-64° with respect to the meridian
- iii) the equatorial 100 and 200 reflections are of weak intensity as compared to the dominant 101 and 201 reflections.

For the structural modeling of the helical assembly of PBI-C10, the same approach was used as in our previous study of the structure determination of the polymer PF2/6.⁶⁵ Rather than taking into account the whole atomic structure of the PBI-C10 molecule to buildup the 21/1 helix, a bead-and-string model was used. Each bead on a strata of the helix represents the center of mass of the pair of PBI-C10 molecules. This implies that the centers of mass of the PBI-C10 pairs are off-centered from the helix axis by a distance corresponding to the helix radius r used as a variable in the modeling (see Figure S5). The off-center character of the helix is ascertained by the strong 101 and 201 reflections and the weak equatorial 100 and 200 reflections.

Our modeling aimed first at determining the helical radius. As seen in Figure 6.a, the most intense reflections close to the 21st layer line are distributed along one line that makes a characteristic angle of 63° with respect to the meridian (see Figure S5). This angle is best reproduced for a model made of helices with a radius of approx. 8 Å.

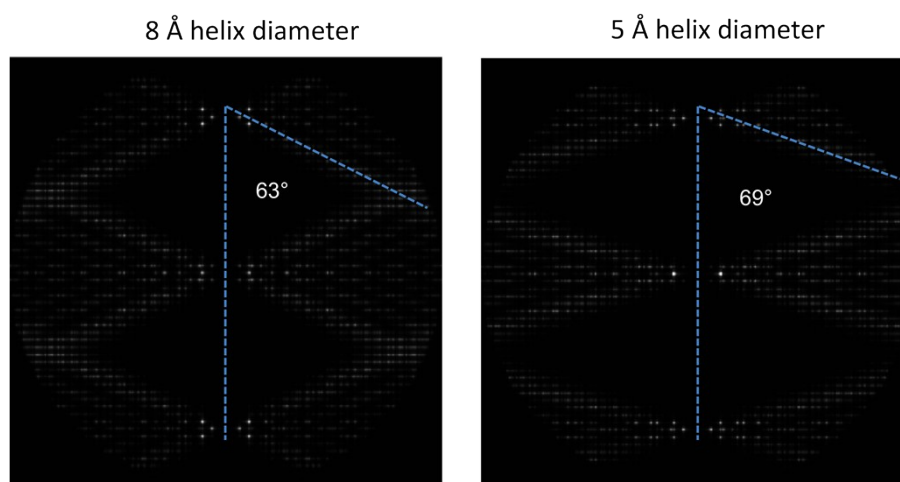


Figure S5. Comparison of the calculated Fiber patterns for a frustrated trigonal structure containing 3 helices. The two patterns correspond to two models made of mathematical helices (bead-and-string model) with a different radius. The dotted lines in the ED patterns highlight the direction of the most intense reflections that is correlated to the helix radius.

Second, the non-meridional position of the reflections in the 21st layer is a characteristic fingerprint of so-called frustrated trigonal structures as evidenced by Lotz and coworkers for numerous polyolefins.⁶⁶⁻⁶⁹ In polymers, the concept of frustration has been introduced and analyzed from a “local” i.e. crystallographic standpoint.¹ In polymeric systems, frustration is often observed when polymer chains with three-fold symmetry are organized in a hexagonal environment. Representative examples of frustrated polymer structures are the alpha form of sPS and the beta form of iPP.¹⁻⁴ In

structures involving three-fold helices, privileged interactions between two helices are observed whereas the third helix probes some discomfort. This latter helix must adopt a specific position and orientation with respect to the two other helices whose relative arrangement is optimized. In general, the third helix is shifted along the helical axis by $c/6$ and has a different azimuthal setting with respect to the other two helices. Indeed, to observe a non meridional intensity distribution in the 21st layer, it is necessary to shift and rotate one helix with respect to the two other helices in the unit cell. Any other packing of three helices based on a higher symmetry such as P3, P3₁ or P3₂ would result in a dominant meridional 0 0 21 reflection (see Figure S6).

To finalize the modeling of the frustrated structure, it was necessary to adjust the offset angle θ of one helix with respect to the two other helices in the unit cell (see Figure 7). The θ angle was refined by trial-and-error to a value of 180° corresponding to the best agreement between calculated and experimental diffraction patterns. The intensity of the off-meridional 1 0 21 reflection and the strong intensities of the 1 0 1, 2 0 1 and 3 0 2 reflections are nicely reproduced in Figure 7.c. The absence of the 1 0 0 and 2 0 0 reflections in the calculated ED results from the use of the bead-and-string model that does not take into account the electronic density of the PBI-C10 molecules present on the helical axis that should contribute to the intensity of the 1 0 0 and 2 0 0 reflections.

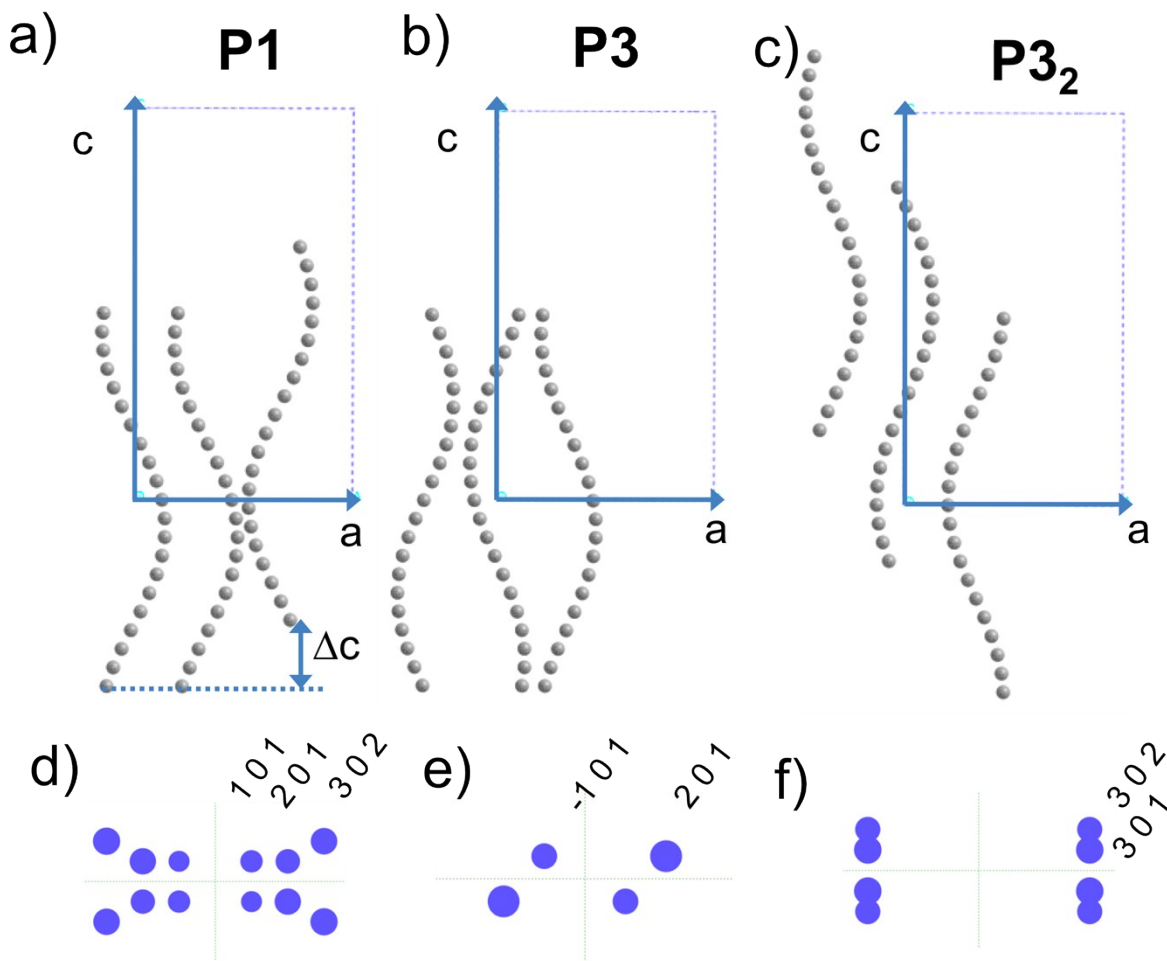


Figure S6. Figure (a)-(c) depict the b-axis projections of the unit cells for the trigonal structures of form II obtained for P1, P3 and P3₂ symmetries, respectively. The corresponding calculated ED patterns are shown in (d)-(f). The unit cells with the P3 and P3₂ symmetry yield calculated ED patterns that show poor agreement with the experimental pattern (the intensities of either the 2 0 1 or the 3 0 1 reflections are overestimated) and both patterns show a dominant meridional 0 0 21 reflection.

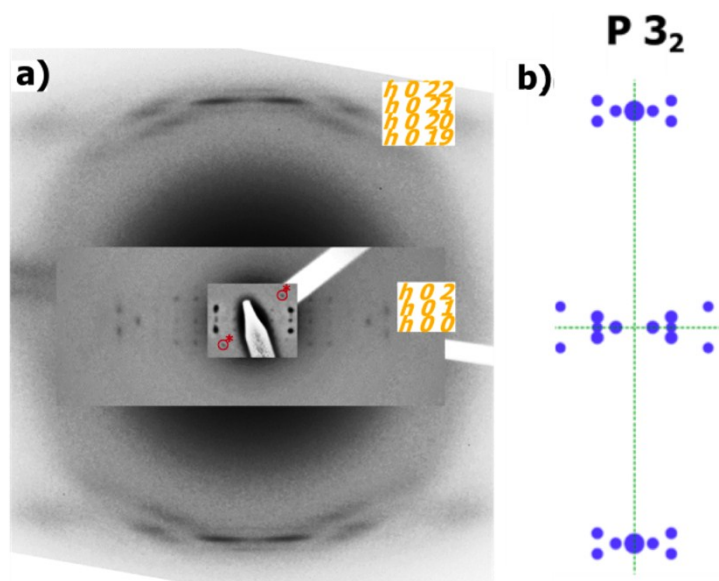


Figure S7. a) Experimental electronic diffraction pattern for a PDI-C10 form II oriented thin film corresponding to a dominant $[0\ 0\ 1]$ zone. The additional reflection indicated by an asterisk corresponds to an extra reflection from a minority population of crystalline domains with a different contact plane. Simulated diffraction patterns for a trigonal structure harboring a triplet of $21_{/1}$ helices using $P\ 3_2$ space groups. Note the strong intensity of the meridional $0\ 0\ 21$ reflection.

References.

- (1) Lotz, B. *Macromolecules* **2012**, 45, 2175-2189.
- (2) Cartier, L.; Okihara, T. and Lotz, B. *Macromolecules* **1998**, 31, 3303-3310.
- (3) (a) Lotz, B.; Kopp, S.; Dorset, D. L. *C. R. Acad. Sci. Paris* **1994**, 319, 187;
- (4) Dorset, D. L. McCourt, M.; Kopp, S.; Shumacher, M.; Okihara, T. and Lotz, B. *Polymer* **1998**, 39, 6331.